General Synthesis of Homoleptic Indium Alkoxide Complexes and the Chemical Vapor Deposition of Indium Oxide Films

Seigi Suh and David M. Hoffman*

Contribution from the Department of Chemistry and the Materials Research Science and Engineering Center, University of Houston, Houston, Texas 77204

Received March 8, 2000

Abstract: A general synthetic route to homoleptic indium alkoxide complexes was developed, and one of the new compounds was used as a precursor to transparent, conductive indium oxide films. The amide complex In[N-*t*-Bu($SiMe_3$)]$_3$ reacted with *t*-BuOH, $EtMe_2COH$, Et_2MeCOH and *i*-$PrMe_2COH$ to yield the dimers [In(μ-OR)(OR)$_2$]$_2$ (R = *t*-Bu, CMe_2Et, $CMeEt_2$, and CMe_2*i*-Pr) in high yield. Similar reactions of In[N-*t*-Bu($SiMe_3$)]$_3$ with the less bulky alcohols *i*-PrOH and Et_2HCOH yielded, respectively, insoluble [In(O-*i*-Pr)$_3$]$_n$ and the tetramer In[(μ-$OCHEt_2$)$_2$In($OCHEt_2$)$_2$]$_3$, which has a six-coordinate central indium atom surrounded by three four-coordinate indium atoms. The compounds [In(O-*i*-Pr)$_3$]$_n$ and In[(μ-$OCHEt_2$)$_2$In($OCHEt_2$)$_2$]$_3$ were also prepared by reacting [In(μ-O-*t*-Bu)(O-*t*-Bu)$_2$]$_2$ with an excess of the respective alcohols. Attempts to prepare the previously reported oxo cluster $In_5(\mu_5\text{-O})(\mu_3\text{-O-}i\text{-Pr})_4(\mu_2\text{-O-}i\text{-Pr})_4(\text{O-}i\text{-Pr})_5$ by thermally decomposing [In(O-*i*-Pr)$_3$]$_n$ failed. The reaction between In[N-*t*-Bu($SiMe_3$)]$_3$ and 2,6-diisopropylphenol afforded the bis *tert*-butylamine adduct In(O-2,6-*i*-$Pr_2C_6H_3$)$_3$(H_2N-*t*-Bu)$_2$. The evidence suggests that the *tert*-butylamine ligands in In(O-2,6-*i*-$Pr_2C_6H_3$)$_3$(H_2N-*t*-Bu)$_2$ resulted from a secondary reaction between HN-*t*-Bu($SiMe_3$) and 2,6-diisopropylphenol. The powerful donor *p*-(dimethylamino)pyridine (*p*-Me_2Npy) reacted with [In(μ-O-*t*-Bu)(O-*t*-Bu)$_2$]$_2$ to yield 5-coordinate In(O-*t*-Bu)$_3$(*p*-Me_2Npy)$_2$ and with the more sterically encumbered complex [In(μ-$OCMeEt_2$)($OCMeEt_2$)$_2$]$_2$ to yield four-coordinate In($OCMeEt_2$)$_3$(*p*-Me_2Npy). In addition, [In(μ-O-*t*-Bu)(O-*t*-Bu)$_2$]$_2$ reacted with 2,2,6,6-tetramethyl-3,5-heptanedione (*t*-Bu_2-β-diketone) to afford (*t*-BuO)$_2$In(μ-O-*t*-Bu)$_2$In(*t*-Bu_2-β-diketonate)$_2$, which has four- and six-coordinate indium centers and virtual C_2 symmetry. X-ray crystallographic studies were carried out for [In(μ-O-*t*-Bu)(O-*t*-Bu)$_2$]$_2$, In[(μ-$OCHEt_2$)$_2$In($OCHEt_2$)$_2$]$_3$, In(O-2,6-*i*-$Pr_2C_6H_3$)$_3$(H_2N-*t*-Bu)$_2$·1/2C_7H_9, In(O-*t*-Bu)$_3$(*p*-Me_2Npy)$_2$·1/2Et_2O, In($OCMeEt_2$)$_3$(*p*-Me_2Npy), and (*t*-BuO)$_2$In(μ-O-*t*-Bu)$_2$In(*t*-Bu_2-β-diketonate)$_2$. The *t*-amoxide complex [In($OCMe_2Et$)$_3$]$_2$ and oxygen were used as precursors to deposit transparent, highly conductive indium oxide films on silicon, glass, and quartz substrates at substrate temperatures of 300−500 °C in a low-pressure chemical vapor deposition process. A backscattering spectrum indicated the film deposited at 500 °C was stoichiometric In_2O_3 (O/In = 1.46 ± 0.07). The films were transparent in the visible region (>75%) and had resistivities as low as 9.1×10^{-4} Ω cm. X-ray diffraction studies indicated the films deposited on glass were cubic and highly (100) oriented.

Indium oxide films are both transparent to visible light and conductive.[1] Dopants (e.g., tin or fluorine) can be used to increase the conductivity of the films and to make them more suitable for applications such as in solid-state optoelectronic devices. Among the methods used to prepare doped and undoped indium oxide films, the technique of chemical vapor deposition (CVD), which in its simplest modification involves the transfer of reagent vapors to a hot substrate for film growth, is the most practical when high throughput of the substrate is a consideration. An important concern in using the CVD method is the choice of the precursor, because it can affect the growth rate, conformality, electrical properties, and transparency of the film. Indium β-diketonate complexes, such as tris(acetylacetonato)-indium, have been the most commonly used precursors to doped and undoped indium oxide films,[2−10] but indium carboxylate,[11−16] alkyl,[17−21] thiolate,[22] and halide[23] complexes have also been studied. None of these precursors is entirely satisfactory. The β-diketonate and carboxylate complexes, for example, are solids

* To whom correspondence should be addressed.

(1) Hartnagel, H. L.; Dawar, A. L.; Jain, A. K.; Jagadish, C. *Semiconducting Transparent Thin Films*; Institute of Physics Publishing: Philadelphia, 1995; and references therein.
(2) Korzo, V. F.; Ryabova, L. A. *Sov. Phys. Solid State* **1967**, *9*, 745.
(3) Ryabova, L. A.; Savitskaya, Ya. S. *J. Vac. Sci. Technol.* **1969**, *6*, 934.
(4) Kane, J. U.S. Patent 3 854 992, 1974.
(5) Kane, J.; Schweizer, H. U.S. Patent 3 944 684, 1976.
(6) Kane, J.; Schweizer, H.; Kern, W. *Thin Solid Films* **1975**, *29*, 155.
(7) Ryabova, L. A.; Salun, V. S.; Serbinov, I. A. *Thin Solid Films* **1982,** *92*, 327.
(8) Maruyama, T.; Fukui, K. *J. Appl. Phys.* **1991**, *70*, 3848.
(9) Nishino, J.; Kawarada, T.; Ohshio, S.; Saitoh, H.; Maruyama, K.; Kamata, K. *J. Mater. Sci. Lett.* **1997**, *16*, 629.
(10) Wang, A.; Dai, J.; Cheng, J.; Chudzik, M. P.; Marks, T. J.; Chang, R. P. H.; Kannewurf, C. R. *Appl. Phys. Lett.* **1998**, *73*, 327.
(11) Xu, J. J.; Shaikh, A. S.; Vest, R. W. *Thin Solid Films* **1988**, *161*, 273.
(12) Maruyama, T.; Fukui, K. *Jpn. J. Appl. Phys.* **1990**, *29*, L1705.
(13) Maruyama, T.; Tabata, K. *Jpn. J. Appl. Phys.* **1990**, *29*, L355.
(14) Maruyama, T.; Fukui, K. *Thin Solid Films* **1991**, *203*, 297.
(15) Maruyama, T.; Nakai, T. *J. Appl. Phys.* **1992**, *71*, 2915.
(16) Hepp, A. F.; Andras, M. T.; Duraj, S. A.; Clark, E. B.; Hehemann, D. G.; Scheiman, D. A.; Fanwick, P. E. *Mater. Res. Soc. Symp. Proc.* **1994**, *335*, 227.
(17) Maruyama, T.; Kitamura, T. *Jpn. J. Appl. Phys.* **1989**, *28*, L1096.
(18) Mayer, B. E. U.S. Patent 5 122 391, 1992.
(19) Melas, A. A. U.S. Patent 5 147 688, 1992.
(20) Mayer, B. *Thin Solid Films* **1992**, *221*, 166.
(21) Ozasa, K.; Ye, T.; Aoyagi, Y. *J. Vac. Sci. Technol. A* **1994**, *12*, 120.

10.1021/ja000845a CCC: $19.00 © 2000 American Chemical Society
Published on Web 09/13/2000

at moderate temperatures, a property that can produce variable precursor delivery to the substrate, and although the alkyl complexes are volatile, they are pyrophoric, which complicates precursor handling. Surprisingly, there are no reports on the use of indium alkoxide complexes as precursors despite the well-accepted general application of metal alkoxide complexes in the preparation of oxide films.

In pursuing the possibility of using indium tris(alkoxide) complexes as precursors to indium oxide, it became apparent that the available synthetic routes to the complexes were not satisfactory and that a new synthetic method would need to be developed. In 1976, Mehrotra and co-workers reported the synthesis of an extensive series of indium tris(alkoxide) compounds, $In(OR)_3$, in which R = Me, Et, *i*-Pr, *n*-Bu, *s*-Bu, *t*-Bu, and pentyl.[24] The isopropoxide complex was prepared by reacting $InCl_3$ with NaO-*i*-Pr in refluxing 2-propanol, and the isolated complex was then used as the starting material to prepare the other alkoxide compounds via alcohol/alkoxide exchange reactions (R = Me, Et, *n*-Bu, *s*-Bu, and pentyl) or transesterification (R = *t*-Bu). The compounds were described as being involatile, and the isopropoxide complex was determined to have a molecular complexity of 4 in boiling 2-propanol. With respect to the latter, Bradley and co-workers[25] later synthesized the oxo-centered cluster $In_5(\mu_5\text{-O})(\mu_3\text{-O-}i\text{-Pr})_4(\mu_2\text{-O-}i\text{-Pr})_4(\text{O-}i\text{-Pr})_5$ by using the same reagents ($InCl_3$ and NaO-*i*-Pr) and reaction conditions similar to those which were reported by Mehrotra. Subsequent work by Bradley et al. suggested that the oxo group in the cluster did not result from water contamination.[26] On the basis of Bradley's reports, it appears probable that Mehrotra's "$In(O\text{-}i\text{-}Pr)_3$" compound is, in fact, an oxo-centered cluster, and the other compounds derived directly from it are not simple homoleptic alkoxide complexes. Several years after the Bradley reports, a patent appeared that described the preparation of "soluble indium alkoxides" by reacting indium trihalides with C_3-C_{20} alcohols in the presence of a strong amine base, such as proton sponge.[27] The illustrative examples provided in the patent, however, are not experimental procedures leading to pure, well-characterized homoleptic indium alkoxide complexes.

In this paper, we describe a general, reliable synthesis of homoleptic indium tris(alkoxide) complexes and the use of one of the new complexes as a precursor to prepare high-quality indium oxide films by CVD at low substrate temperatures.

Results and Discussion

Synthesis. Schemes 1 and 2 summarize most of the synthetic results. The development of the synthetic route to the alkoxide complexes was dependent on the use of $In[N\text{-}t\text{-}Bu(SiMe_3)]_3$ as the starting material. $In[N\text{-}t\text{-}Bu(SiMe_3)]_3$, which was prepared in moderate yield from $InCl_3$ and $LiN\text{-}t\text{-}Bu(SiMe_3)$ following the procedure of Kim et al.,[28] is a rare example of a well-characterized homoleptic indium amide complex.[29,30]

Scheme 1

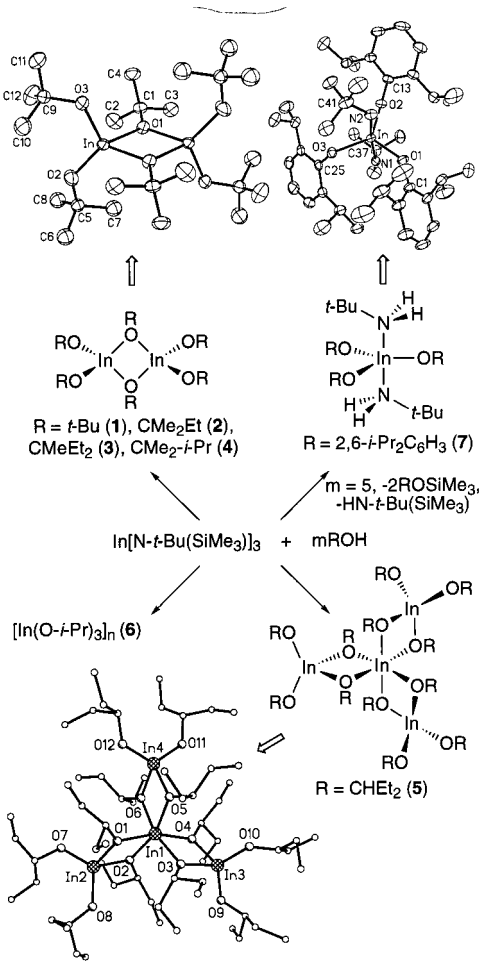

The amide complex $In[N\text{-}t\text{-}Bu(SiMe_3)]_3$ reacted with *t*-BuOH, $EtMe_2COH$, Et_2MeCOH, and *i*-$PrMe_2COH$ to yield the dimers $[In(\mu\text{-OR})(OR)_2]_2$ [R = *t*-Bu (**1**), CMe_2Et (**2**), $CMeEt_2$ (**3**), and CMe_2-*i*-Pr (**4**)] and with Et_2HCOH to afford the tetramer $In[(\mu\text{-}OCHEt_2)_2In(OCHEt_2)_2]_3$ (**5**). It was necessary to use excess alcohol in the reactions involving the two bulky alcohols, Et_2MeCOH and *i*-$PrMe_2COH$, because the reactions with stoichiometric amounts were slow to go to completion. Compound **5** was also prepared cleanly by reacting **1** with excess 3-pentanol in hexanes (eq 1).

$$2[In(\mu\text{-O-}t\text{-Bu})(\text{O-}t\text{-Bu})_2]_2 + 12Et_2HCOH \rightarrow In[(\mu\text{-}OCHEt_2)_2In(OCHEt_2)_2]_3 + 12t\text{-BuOH} \quad (1)$$

Two other amide complexes,[29,30] $In(tmp)_3$ (tmp = 2,2,6,6-tetramethylpiperidino) and $In(NEt_2)_3$, were tested as alternatives to $In[N\text{-}t\text{-}Bu(SiMe_3)]_3$ for the preparation of **1**. The reactions produced **1** in about the same yield as when $In[N\text{-}t\text{-}Bu(SiMe_3)]_3$ was used. Overall, however, $In[N\text{-}t\text{-}Bu(SiMe_3)]_3$ is a better choice for starting material than $In(tmp)_3$ because the yield of $In(tmp)_3$ is less than the yield of $In[N\text{-}t\text{-}Bu(SiMe_3)]_3$ (based on $InCl_3$) and $HN\text{-}t\text{-}Bu(SiMe_3)$ is less expensive than Htmp. In the case of $In(NEt_2)_3$, the amide itself is difficult to isolate and purify and, therefore, is not as convenient to use as $In[N\text{-}t\text{-}Bu(SiMe_3)]_3$.

Compounds **3** and **4** sublimed cleanly at <150 °C in vacuo while **1** sublimed in vacuo at ≈130 °C with some decomposition. Compound **2** became a liquid at around 40 °C and condensed on the coldfinger of the sublimer as a solid. All the compounds were very soluble in hexanes and benzene. The

(22) Nomura, R.; Konishi, K.; Matsuda, H. *J. Electrochem. Soc.* **1991**, *138*, 631.
(23) Kawamata, E.; Ohshima, K. *Jpn. J. Appl. Phys.* **1979**, *18*, 205.
(24) Chatterjee, S.; Bindal, S. R.; Mehrotra, R. C. *J. Indian Chem. Soc.* **1976**, *53*, 867.
(25) Bradley, D. C.; Chudzynska, H.; Frigo, D. M.; Hursthouse, M. B.; Mazid, M. A. *J. Chem. Soc., Chem. Commun.* **1988**, 1258.
(26) Bradley, D. C.; Chudzynska, H.; Frigo, D. M.; Hammond, M. E.; Hursthouse, M. B.; Mazid, M. A. *Polyhedron* **1990**, *9*, 719.
(27) Moore, C. P.; Wettling, D. M. U.S. Patent 5 237 081, 1993.
(28) Kim, J.; Bott, S. G.; Hoffman, D. M. *Inorg. Chem.* **1998**, *37*, 3835.
(29) Frey, R.; Gupta, V. D.; Linti, G. *Z. Anorg. Allg. Chem.* **1996**, *622*, 1060.
(30) Rossetto, G.; Brianese, N.; Camporese, A.; Porchia, M.; Zanella, P.; Bertoncello, R. *Main Group Met. Chem.* **1991**, *14*, 113.

Scheme 2

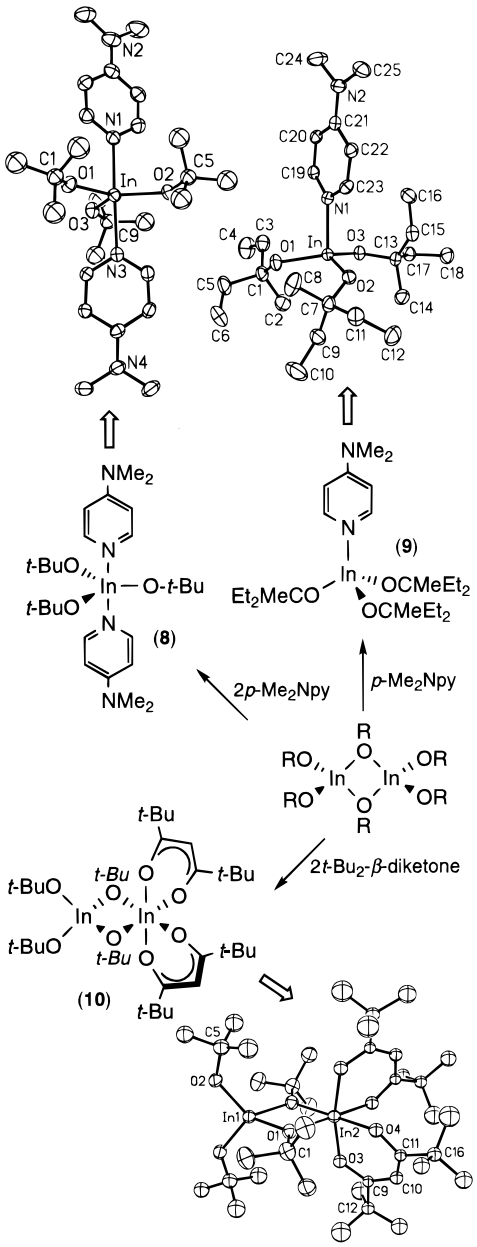

NMR spectra for **1**−**5** are consistent with the structures shown in Scheme 1.

Reactions of In[N-*t*-Bu(SiMe$_3$)]$_3$ with *i*-PrOH yielded an insoluble white solid as the product. A chemical analysis (C, H, and N) of the solid was consistent with the empirical formula In(O-*i*-Pr)$_3$ (**6**). Compound **6** was also prepared by reacting **1** with excess 2-propanol in benzene according to eq 2. Infrared spectroscopy was used to verify that **6** was the product of eq 2. All attempts to dissolve **6** in a variety of solvents, including pyridine and hot 2-propanol, failed. On this basis, the compound is proposed to be polymeric, [In(O-*i*-Pr)$_3$]$_n$, perhaps with six-coordinate In centers as in [In(μ-SePh)$_3$]$_\infty$.[31]

$$n/2[\text{In}(\mu\text{-O-}t\text{-Bu})(\text{O-}t\text{-Bu})_2]_2 + 3n\,i\text{-PrOH} \rightarrow [\text{In}(\text{O-}i\text{-Pr})_3]_n + 3n\,t\text{-BuOH} \quad (2)$$

To test whether **6** could be a precursor to the cluster In$_5$(μ_5-O)(μ_3-O-*i*-Pr)$_4$(μ_2-O-*i*-Pr)$_4$(O-*i*-Pr)$_5$, a small sample of **6** was heated in refluxing 2-propanol, the conditions under which the oxo cluster was formed from InCl$_3$ and NaO-*i*-Pr by Bradley et al.[25,26] After refluxing for 2 h, the 2-propanol was distilled in vacuo, and the residue was dried thoroughly in vacuo and then extracted with C$_6$D$_6$. A ^{1}H NMR spectrum of the extract did not have any of the resonances previously reported for a C$_6$D$_6$ solution of In$_5$(μ_5-O)(μ_3-O-*i*-Pr)$_4$(μ_2-O-*i*-Pr)$_4$(O-*i*-Pr)$_5$.[25,26] Thus, **6** is not converted to In$_5$(μ_5-O)(μ_3-O-*i*-Pr)$_4$(μ_2-O-*i*-Pr)$_4$(O-*i*-Pr)$_5$ under reaction conditions similar to those used by Bradley and co-workers to prepare the oxo cluster (but without the presence of InCl$_3$, NaO-*i*-Pr, and products derived from these reagents).

The reaction between In[N-*t*-Bu(SiMe$_3$)]$_3$ and 2,6-diisopropylphenol takes a different course from those involving the other alcohols. The amide complex In[N-*t*-Bu(SiMe$_3$)]$_3$ reacted with 3 equiv of 2,6-diisopropylphenol to yield the bis-*tert*-butylamine adduct In(O-2,6-*i*-Pr$_2$C$_6$H$_3$)$_3$(H$_2$N-*t*-Bu)$_2$ (**7**) rather than the expected homoleptic phenoxide complex. By using the required 5 equiv of 2,6-diisopropylphenol instead of 3 (eq 3), the yield of **7** was increased from 39% to 53% (based on In).

$$\text{In[N-}t\text{-Bu(SiMe}_3\text{)]}_3 + 5i\text{-Pr}_2\text{-2,6-C}_6\text{H}_3\text{OH} \rightarrow \text{In(O-2,6-}i\text{-Pr}_2\text{C}_6\text{H}_3\text{)}_3\text{(H}_2\text{N-}t\text{-Bu)}_2 + 2i\text{-Pr}_2\text{-2,6-C}_6\text{H}_3\text{OSiMe}_3 + \text{HN-}t\text{-Bu(SiMe}_3\text{)} \quad (3)$$

The apparent disruption of the amide ligands in In[N-*t*-Bu(SiMe$_3$)]$_3$ is not unique to the reaction to form **7**. Similar occurrences[32] were observed in reactions between In[N-*t*-Bu(SiMe$_3$)]$_3$ and the acidic fluorinated alcohols (CF$_3$)$_2$MeCOH and (CF$_3$)$_2$CHOH (pK_a = 9.6 and 9.3,[33] respectively), but ligand breakdown was not observed[32,34] in reactions involving the less acidic reagents (CF$_3$)Me$_2$COH (pK_a ≈ 14−15)[33] and alkylthiols (pK_a ≈ 12).[35] To test whether 2,6-*i*-Pr$_2$C$_6$H$_3$OH (pK_a ≈ 10−11) reacts with Me$_3$Si(*t*-Bu)NH without the presence of indium, 2,6-*i*-Pr$_2$C$_6$H$_3$OH and Me$_3$Si(*t*-Bu)NH were mixed in an NMR tube (benzene-d_6 solvent, ≈1:1 stoichiometry) and the reaction was monitored by ^{1}H NMR spectroscopy. The NMR data were consistent with the reaction producing *t*-BuNH$_2$ and 2,6-*i*-Pr$_2$C$_6$H$_3$OSiMe$_3$ (eq 4), which probably occurs via the intermediate [H$_2$N-*t*-Bu(SiMe$_3$)][O-2,6-*i*-Pr$_2$C$_6$H$_3$] (not observed). This result suggests that the secondary reaction shown in eq 4 is the source of the *t*-BuNH$_2$ ligands in **7**. If the generation of *t*-BuNH$_2$ is to be avoided in reactions between In[N-*t*-Bu(SiMe$_3$)]$_3$ and X−H reagents, the present results and our previous observations put a lower limit on the pK_a(X−H) of approximately 10−11.

$$\text{Me}_3\text{Si(}t\text{-Bu)NH} + \text{2,6-}i\text{-Pr}_2\text{C}_6\text{H}_3\text{OH} \rightleftharpoons t\text{-BuNH}_2 + \text{2,6-}i\text{-Pr}_2\text{C}_6\text{H}_3\text{OSiMe}_3 \quad (4)$$

Attempts to grow X-ray crystallographic-quality crystals of any of the [In(μ-OR)(OR)$_2$]$_2$ derivatives failed initially. For this reason, monomeric Lewis base adducts were prepared from the dimer compounds. The expectation was that the monomeric compounds would produce higher quality crystals (Scheme 2). Compound **1** reacted with 2 equiv of the powerful donor *p*-(dimethylamino)pyridine (*p*-Me$_2$Npy) per indium to yield 5-coordinate In(O-*t*-Bu)$_3$(*p*-Me$_2$Npy)$_2$ (**8**). An attempt to prepare the four-coordinate complex In(O-*t*-Bu)$_3$(*p*-Me$_2$Npy) by using 1 equiv of *p*-Me$_2$Npy per indium yielded **8** and unreacted

(31) Annan, T. A.; Kumar, R.; Mabrouk, H. E.; Tuck, D. G.; Chadha, R. K. *Polyhedron*, **1989**, *8*, 865.

(32) Mîinea, L. A.; Suh, S.; Hoffman, D. M. *Inorg. Chem.* **1999**, *38*, 4447.

(33) Willis, C. J. *Coord. Chem. Rev.* **1988**, *88*, 133.

(34) Suh, S.; Hoffman, D. M. *Inorg. Chem.* **1998**, *37*, 5823.

(35) Lowry, T. H.; Richardson, K. S. *Mechanism and Theory in Organic Chemistry*; Harper & Row: New York, 1976; pp 149−150.

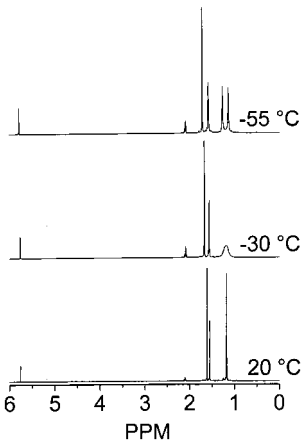

Figure 1. ^{1}H NMR spectra recorded at and below room temperature for (*t*-BuO)$_2$In(μ-O-*t*-Bu)$_2$In(*t*-Bu$_2$acac)$_2$ (**10**) (300 MHz, toluene-d_8). Integration showed that the two peaks centered at 1.6 ppm arising from the O-*t*-Bu ligands are of equal intensity. The resonance at δ 1.2 in the spectrum recorded at 20 °C is due to the methyl groups of the Me_3-CC(O)CHC(O)CMe_3 ligand, and the resonance at δ 2.1 is due to the toluene-d_8 solvent.

starting material. Conversely, 1 or 2 equiv (per indium) of *p*-Me$_2$Npy reacted with the bulkier alkoxide complex **3** to form four-coordinate In(OCMeEt$_2$)$_3$(*p*-Me$_2$Npy) (**9**). In contrast to these results, pyridine adducts of **1**−**4** could not be isolated by mixing **1**−**4** with excess pyridine in diethyl ether followed by removal of diethyl ether and excess pyridine under vacuum. Apparently, pyridine is not a powerful enough donor to allow isolation of adducts. X-ray crystallographic studies of both **8** and **9** were carried out (see below).

In an attempt to form a mixed alkoxide−acetoacetonate complex for possible use as a film precursor, **1** was reacted with 2,2,6,6-tetramethyl-3,5-heptanedione (*t*-Bu$_2$-β-diketone) (Scheme 2). The reaction yielded the diindium complex (*t*-BuO)$_2$In(μ-O-*t*-Bu)$_2$In(*t*-Bu$_2$-β-diketonate)$_2$ (**10**). Proton NMR spectra of **10** recorded in the temperature range −55 to +20 °C (Figure 1) indicated the molecule is fluxional. The temperature dependence exhibited in the *Me*$_3$CC(O)CHC(O)C*Me*$_3$ region of the ^{1}H NMR spectra is consistent with a process that renders the two halves of the *t*-Bu$_2$-β-diketonate ligand equivalent ($\Delta G^\dagger$ = 12 kcal/mol at T_c = −30 °C).[36] A Bailar twist[37] or Ray−Dutt rearrangement at the octahedral center,[38,39] or an In−OR$_{bridge}$ or an In−O(acac) bond cleavage at the octahedral center with subsequent rearrangement at the resultant 5-coordinate In center, could explain the temperature-dependent NMR data. A rapid equilibrium between **10** and its constituent fragments In(O-*t*-Bu)$_3$ and In(*t*-Bu$_2$-β-diketonate)$_2$(O-*t*-Bu) can be excluded as an explanation, because this process would make the terminal and bridge alkoxide ligands equivalent as well. Interestingly, the related aluminum compounds [Al(OR)$_2$(R′$_2$-β-diketonate)]$_2$ (R = $SiMe_3$, *i*-Pr, or *t*-Bu, R′ = Me; R = $SiMe_3$ or *i*-Pr, R′ = Et) are reported to be rigid over the temperature range −60−120 °C.[40]

X-ray Crystallographic Studies. Crystal structures of **1**, **5**, **7** (Scheme 1), **8**, **9**, and **10** (Scheme 2) were carried out. The thermal ellipsoid plots in Schemes 1 and 2 are shown with 40% equiprobability envelopes and with hydrogens omitted. In those compounds having disordered ligands (**1**, **5**, **8**, and **10**), only one orientation of the disordered ligand is shown. Crystallographic data are presented in Table 1, and selected bond distances and angles are given in Tables 2 (**1**, **7**, **8**, **9**, and **10**) and 3 (**5**). The view of **5** in Scheme 1 emphasizes the distortion of the "chelated" central indium atom from an octahedral geometry toward a trigonal prismatic geometry. The twist angle between the triangles defined by the projections of O1, O3, O5 and O2, O4, O6 onto a plane is around 40°. The structures of **5** and **10** are closely related to those of the aluminum complexes[41] Al[(μ-O-*i*-Pr)$_2$Al(O-*i*-Pr)$_2$]$_3$ and (Me$_3$SiO)$_2$Al(μ-OSiMe$_3$)$_2$Al(acac)$_2$,[40,42] respectively.

Compounds **7** and, to a lessor extent, **8** can be described as having trigonal bipyramidal geometries with the pyridine ligands occupying the apical positions. For **7**, the angles in the trigonal plane fall in the narrow range of 117−125° and N1−In−N2 = 173°. This contrasts with **8**, where the angles in the trigonal plane span a much wider range, 99−139°, and N1−In−N3 = 177°. The large angle variation for **8** is caused by steric interactions among the *tert*-butyl substituents, whose tertiary carbons all lie near the trigonal plane (variations from the In/O1/O2/O3 plane for C1, C5, and C9 are −0.18, 0.14, and −0.04, Å, respectively). The largest O−In−O angle in the trigonal plane of **8** involves O1 and O2, which have their respective *tert*-butyl groups pointing at each other, while the smallest angle involves O1 and O3, which have the *tert*-butyl substituents pointing in opposite directions. Similar steric problems are avoided in **7** by folding the phenyl groups above and below the trigonal plane (deviations from the In/O1/O2/O3 plane for C1, C13, and C25 are 0.61, −1.05, and 1.05, respectively). The structure of **9** can be described as trigonal pyramidal with some distortion toward a tetrahedral geometry. The indium atom and O1, O2, and O3 are almost planar ($\sum$O−In−O = 351°) while the N−In−O angles range from 96 to 103°. The geometry closely resembles that of In(S-*t*-Bu)$_3$(py).[34]

The In−OR$_{terminal}$ and In−OR$_{bridge}$ distances in the new complexes are not unusual.[25,26,32,43−47] The In−N distance in **9** is about 0.1 Å shorter than the In−N distances in **7** and **8** and is shorter than most previously observed In−N(amine) distances [2.200(19)-2.408(7) Å].[28,31,32,34,48−55] It is tempting to ascribe the short In−N distance in **9** to the enhanced donor ability of

(36) Martin, M. L.; Delpuech, J.-J.; Martin, G. J. *Practical NMR Spectroscopy*; Heyden: Philadelphia, 1980; Chapter 8.1.2.
(37) Bailar, J. C. *J. Inorg. Nucl. Chem.* **1958**, *8*, 165.
(38) Ray, P.; Dutt, N. K. *J. Indian Chem. Soc.* **1943**, *20*, 81.
(39) Shriver, D.; Atkins, P. *Inorganic Chemistry*, 3rd ed.; W. H. Freeman and Co.: New York, 1999; p 484.
(40) Wengrovius, J. H.; Garbauskas, M. F.; Williams, E. A.; Going, R. C.; Donahue, P. E.; Smith, J. F. *J. Am. Chem. Soc.* **1986**, *108*, 982.
(41) Folting, K.; Streib, W. E.; Caulton, K. G.; Poncelet, O.; Hubert-Pfalzgraf, L. G. *Polyhedron* **1991**, *10*, 1639. Turova, N. Ya.; Kozunov, V. A.; Yanovskii, A. I.; Bokii, N. G.; Struchkov, Yu. T.; Tarnopol'skii, B. L. *J. Inorg. Nucl. Chem.* **1979**, *41*, 5. Shiner, V. J., Jr.; Whittaker, D.; Fernandez, V. P. *J. Am. Chem. Soc.* **1963**, *85*, 2318.
(42) Garbauskas, M. F.; Wengrovius, J. H.; Going, R. C.; Kasper, J. S. *Acta Crystallogr. C* **1984**, *40*, 1536.
(43) Trentler, T. J.; Goel, S. C.; Hickman, K. M.; Viano, A. M.; Chiang, M. Y.; Beatty, A. M.; Gibbons, P. C.; Buhro, W. E. *J. Am. Chem. Soc.* **1997**, *119*, 2172.
(44) Bradley, D. C.; Frigo, D. M.; Hursthouse, M. B.; Hussain, B. *Organometallics* **1988**, *7*, 1112.
(45) Self, M. F.; McPhail, A. T.; Wells, R. L. *J. Coord. Chem.* **1993**, *29*, 27.
(46) Dembowski, U.; Pape, T.; Herbst-Irmer, R.; Pohl, E.; Roesky, H. W.; Sheldrick, G. M. *Acta Crystallogr. C* **1993**, *49*, 1309.
(47) Rose, D. J.; Chang, Y. D.; Chen, Q.; Kettler, P. B.; Zubieta, J. *Inorg. Chem.* **1995**, *34*, 3973.
(48) Jeffs, S. E.; Small, R. W. H.; Worrall, I. J. *Acta Crystallogr. C* **1984**, *40*, 1329.
(49) Small, R. W. H.; Worrall, I. J. *Acta Crystallogr. C* **1982**, *38*, 932.
(50) Leman, J. T.; Roman, H. A.; Barron, A. R. *J. Chem. Soc., Dalton Trans.* **1992**, 2183.
(51) Atwood, D. A.; Jones, R. A.; Cowley, A. H.; Bott, S. G.; Atwood, J. L. *J. Organomet. Chem.* **1992**, *434*, 143.
(52) Atwood, D. A.; Cowley, A. H.; Jones, R. A.; Atwood, J. L.; Bott, S. G. *J. Coord. Chem.* **1992**, *26*, 293.
(53) Veith, M.; Recktenwald, O. *J. Organomet. Chem.* **1984**, *264*, 19.

Table 1. Crystal data for [In(μ-O-*t*-Bu)(O-*t*-Bu)$_2$]$_2$ (**1**), In[(μ-OCHEt$_2$)$_2$In(OCHEt$_2$)$_2$]$_3$ (**5**), [In(O-2,6-*i*-Pr$_2$C$_6$H$_3$)$_3$(H$_2$N-*t*-Bu)$_2$]$_2$·1/2C$_7$H$_9$ (**7**·1/2C$_7$H$_9$), In(O-*t*-Bu)$_3$(*p*-Me$_2$Npy)$_2$·1/2Et$_2$O (**8**·Et$_2$O), In(OCMeEt$_2$)$_3$(*p*-Me$_2$Npy) (**9**), and (*t*-BuO)$_2$In(μ-O-*t*-Bu)$_2$In(*t*-Bu$_2$-β-diketonate)$_2$ (**10**)

	1	**5**	**7**·1/2C$_7$ H$_8$	**8**·1/2C$_4$H$_{10}$O	**9**	**10**
formula	C$_{24}$H$_{54}$O$_6$In$_2$	C$_{60}$H$_{132}$O$_{12}$In$_4$	C$_{44}$H$_{73}$N$_2$O$_3$In ·1/2C$_7$H$_8$	C$_{26}$H$_{47}$N$_4$O$_3$In ·1/2C$_4$H$_{10}$O	C$_{25}$H$_{49}$N$_2$O$_3$In	C$_{38}$H$_{74}$O$_8$In$_2$
fw	668.31	1504.94	838.93	615.56	540.48	888.61
crystal dimens (mm)	0.45 × 0.25 × 0.15	0.40 × 0.35 × 0.12	0.35 × 0.30 × 0.25	0.35 × 0.26 × 0.14	0.35 × 0.25 × 0.15	0.40 × 0.12 × 0.12
space group	*P*-1 (triclinic)	*P*2$_1$/*c* (monoclinic)	*C*2/*c* (monoclinic)	*P*-1(triclinic)	*P*2$_1$/*c* (monoclinic)	*C*2/*c* (monoclinic)
a, Å	9.8502(9)	12.1119(6)	24.1308(13)	9.8335(6)	14.4944(8)	19.6229(11)
b, Å	9.8632(8)	13.5007(7)	12.6401(7)	11.4492(7)	16.2071(9)	11.9153(7)
c, Å	10.0719(9)	45.6039(24)	32.2968(18)	15.4315(9)	12.6679(7)	19.3000(11)
α, deg	73.423(1)			111.581(1)		
β, deg	69.357(1)	96.723(1)	102.8350(10)	90.335(1)	107.677(1)	98.961(1)
γ, deg	61.209(1)			93.682(1)		
T, °C	−50(2)	−50(2)	−50(2)	−50(2)	−50(2)	−50(2)
Z	1	4	8	2	4	4
V, Å^3	794.51(12)	7405.8(7)	3493.9(6)	1611.43(17)	2835.3(3)	4457.5(4)
D_{calcd}, g/cm^3	1.397	1.350	1.160	1.269	1.266	1.324
μ, mm^{-1}	1.481	1.279	0.530	0.767	0.858	1.077
R, R_w[a]	0.0383, 0.0993[b]	0.0426, 0.1012[c]	0.0212, 0.0511[d]	0.0344, 0.0895[e]	0.0193, 0.0505[f]	0.0318, 0.0809[g]

[a] $R = \sum||F_o| - |F_c||/\sum|F_o|$; $R_w = [\sum w(F_o^2 - F_c^2)^2/\sum w(F_o^2)^2]^{1/2}$, $w = [\sigma^2(F_o^2) + (aP)^2 + (bP)]^{-1}$ where $P = (F_o^2 + 2F_c^2)/3$. [b] $a = 0.0575$, $b = 1.7753$. [c] $a = 0.0239$, $b = 33.6848$. [d] $a = 0.0152$, $b = 11.4445$. [e] $a = 0.0439$, $b = 3.1089$. [f] $a = 0.0218$, $b = 1.7653$. [g] $a = 0.0362$, $b = 20.5820$.

Table 2. Selected Bond Distances (Å) and Angles (deg) for [In(μ-O-*t*-Bu)(O-*t*-Bu)$_2$]$_2$ (**1**), [In(O-2,6-*i*-Pr$_2$C$_6$H$_3$)$_3$(H$_2$N-*t*-Bu)$_2$]$_2$ (**7**), In(O-*t*-Bu)$_3$(*p*-Me$_2$Npy)$_2$ (**8**), In(OCMeEt$_2$)$_3$(*p*-Me$_2$Npy) (**9**), and (*t*-BuO)$_2$In(μ-O-*t*-Bu)$_2$In(*t*-Bu$_2$-β-diketonate)$_2$ (**10**)

	1	**7**	**8**	**9**	**10**
			Distances		
In−O1	2.115(3)	2.0751(14)	2.027(2)	2.0139(16)	2.100(3)
In−O2	1.969(4)	2.0569(14)	2.058(2)	2.0153(15)	1.993(3)
In−O3	1.985(4)	2.0627(15)	2.037(2)	2.0282(15)	
In−O1′	2.107(3)				
In−N1		2.3098(18)	2.347(3)	2.2138(18)	
In−N(*n*)		2.3093(19) (*n* = 2)	2.328(3) (*n* = 3)		
In2−O1					2.152(3)
In2−O3					2.131(5)
In2−O4					2.152(6)
			Angles		
O1−In−O2	119.84(17)	116.74(6)	138.59(10)	116.27(7)	118.94(13)
O1−In−O3	106.97(15)	118.17(6)	99.42(11)	119.04(6)	
O2−In−O3	117.25(16)	125.00(6)	121.95(10)	115.51(6)	
O1′−In-O2	119.41(18)				118.79(13)
O1′−In-O3	109.45(15)				
O1−In−O1′	77.05(13)				77.00(16)
O2−In−O2′					103.82(18)
O1−In2−O4					99.3(3)
O3−In2−O4					91.3(3)
O1−In2−O4′					173.4(2)
O3−In2−O3′					166.8(4)
O3−In2−O4′					79.1(3)
O4−In2−O4′					86.7(5)
In−O1−In	102.95(13)				104.09(12)
O1−In2−O1′					74.81(16)
N1−In−O1		91.71(7)	87.74(11)	100.72(7)	
N1−In−O2		90.79(6)	90.16(10)	96.37(7)	
N1−In−O3		90.50(7)	90.15(11)	103.31(7)	
N(*n*)−In−O1		81.94(7) (*n* = 2)	94.68(10) (*n* = 3)		
N(*n*)−In−O2		90.30(7) (*n* = 2)	88.50(10) (*n* = 3)		
N(*n*)−In−O3		94.25(7) (*n* = 2)	88.74(11) (*n* = 3)		
N1−In−N(*n*)		173.34(8) (*n* = 2)	177.47(10) (*n* = 3)		

p-Me$_2$Npy as compared to normal amine ligands, but the distances in five-coordinate In(S-*i*-Pr)$_3$(*p*-Me$_2$Npy)$_2$ [2.405(3) Å][34] and four-coordinate In[N-*t*-Bu(SiHMe$_2$)]$_3$(*p*-Me$_2$Npy) [2.327(3) Å][28] are not shorter than normal.

Chemical Vapor Deposition Studies. Volatile liquid precursors are preferred over solid precursors when depositing films by CVD, because liquids can be delivered at a uniform rate to the substrate by using simple, inexpensive bubblers and mass

(54) Bradley, D. C.; Dawes, H.; Frigo, D. M.; Hursthouse, M. B.; Hussain, B. J. *Organomet. Chem.* **1987**, *325*, 55.

(55) Kühner, S.; Hausen, H.-D.; Weidlein, J. Z. *Anorg. Allg. Chem.* **1998**, *624*, 13.

Table 3. Selected Bond Distance (Å) and Angle (deg) Ranges for $In[(\mu\text{-}OCHEt_2)_2In(OCHEt_2)_2]_3$ (**5**)

Distances	
In1−O	2.166(4)−2.182(4)
$In(2-4)-O_{bridge}$	2.091(4)−2.100(4)
$In(2-4)\text{-}O_{term}$	1.974(5)−2.001(5)
Angles	
$O(n)-In1-O(n+1)$ $n = 1, 3, 5$	73.62(14)−74.16(15)
O−In1−O[a]	91.70(16)−101.52(15)
$O(n)-In1-O(n+3)$ $n = 1, 2, 3$	160.71(15)−164.39(15)
$In1-O_{bridge}-In$	104.02(16)−104.72(15)
$O_{term}-In(2-4)-O_{term}$	122.2(2)−124.0(3)
$O_{bridge}-In(2-4)-O_{bridge}$	76.60(15)−77.38(15)
$O_{term}-In(2-4)-O_{bridge}$	107.33(19)−115.1(2)

[a] Angles exo to four-membered $In(\mu\text{-}O)_2In$ rings.

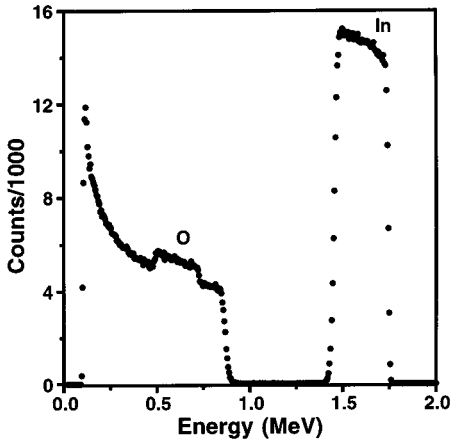

Figure 2. Rutherford backscattering (RBS) spectrum for an indium oxide film deposited on silicon at 500 °C.

flow controllers. Thermal stability in the heated bubbler is also vitally important to ensure a constant delivery rate. Of the new homoleptic alkoxide compounds and their derivatives prepared in this study, the *t*-amoxide complex **2** was the most viable precursor candidate, because it liquified at moderate temperatures (mp 40−41 °C), and it could be distilled without decomposition.

Compound **2** and dry O_2 reacted to yield shiny, adherent films in a low-pressure CVD process at substrate temperatures of 300−500 °C. An analysis of the Rutherford backscattering (RBS) spectrum for a film deposited at 500 °C (Figure 2) indicated that within experimental error the stoichiometery was In_2O_3 (O/In = 1.46 ± 0.07). A carbon peak was not observed in the spectrum, indicating low carbon contamination levels (<1 atom %). After sputtering into the bulk, the X-ray photoelectron spectrum for a film deposited on silicon at 500 °C showed In $3d_{5/2}$ and $3d_{3/2}$ peaks at 445.11 and 452.59 eV, respectively, and the O 1*s* peak at 530.56 eV. Values of 444.8 and 452.6 eV for In $3d_{5/2}$ and $3d_{3/2}$, respectively, and 530.4 for O 1*s* have been reported previously.[56,57] A complete XPS depth profile for a film deposited at 460 °C on silicon indicated there was virtually no carbon in the films.

Film growth rates, which were calculated from film thicknesses obtained by cross-sectional scanning electron microscopy (SEM), increased from 110 Å/min at T_{dep} = 300 °C to 430 Å/min at T_{dep} = 500 °C (Table 4), all at constant bubbler and feed-line temperatures. Although growth rates were not optimized, higher growth rates were observed when the bubbler

Table 4. Growth Rates and Resistivities of Films Deposited on Silicon from $[In(\mu\text{-}OCMe_2Et)(OCMe_2Et)_2]_2$ (**2**) and Oxygen

dep temp (°C)	growth rate[a] (Å/min)	resistivity[b] (× 10^{-4} Ω cm)
300	110	10.7
340	190	9.9
380	260	9.9
420	300	9.8
460	350	9.1
500	430	10.1

[a] Constant bubbler and feed-line temperatures. [b] The error is estimated to be ±3%.

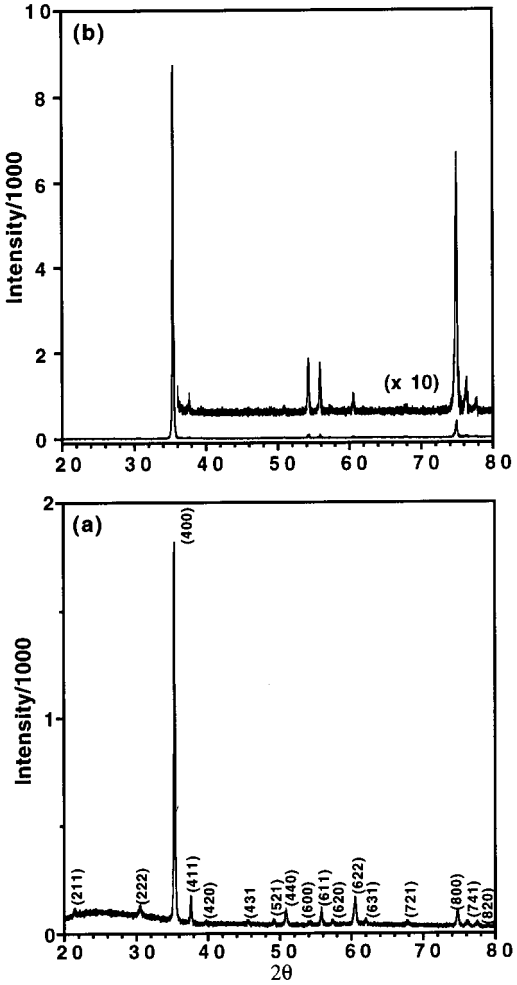

Figure 3. X-ray diffraction patterns for 3600- (a) and 13 000-Å (b) films deposited on glass at 460 °C.

temperature was increased; for example, when the bubbler was heated to 70 °C, the growth rate increased nearly 5-fold at T_{dep} = 460 °C. The highest growth rate for CVD indium oxide films, ≈8000 Å/min, has been reported by Mayer, who used pyrophoric trimethylindium diethyl etherate, $InMe_3(OEt_2)$, and oxygen precursors in an atmospheric pressure CVD process.[20]

X-ray diffraction studies on ≈3600-Å films deposited at 300−500 °C on glass indicated the films were composed of (100)-oriented cubic indium oxide (e.g., Figure 3a). The diffraction spectra did not change significantly with deposition temperature. The films were more oriented, however, as the film thickness was increased (Figure 3b). This suggests there is a buffering effect from the initial growth of textured material on the glass substrate.

Micrographs for films (3000−3600 Å) deposited at 300−500 °C on silicon indicated that the films had textured domains

(56) Jeong, J. I.; Moon, J. H.; Hong, J. H.; Kang, J.; Fukuda, Y.; Lee, Y. P. *J. Vac. Sci. Technol. A* **1996**, *14*, 293.
(57) Barr, T. L.; Liu, Y. L. *J. Phys. Chem. Solids* **1989**, *50*, 657.

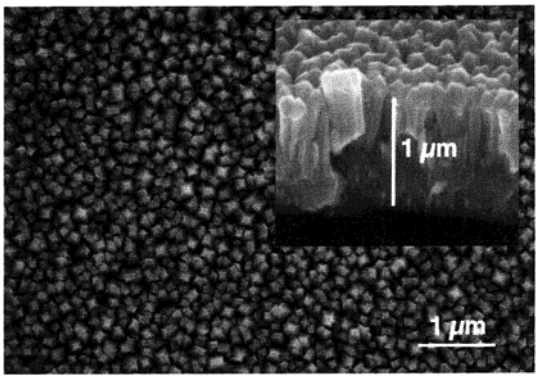

Figure 4. Surface SEM image and cross sectional view (inset: 60° tilt angle) of a 13 000-Å film deposited on silicon at 460 °C.

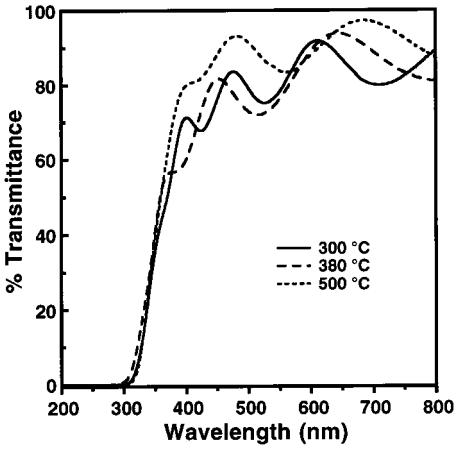

Figure 5. UV−vis spectra for films deposited on quartz at 300, 380, and 500 °C.

with no discernible cracks. Comparison of the surface morphologies of 3600 and 13 000-Å films (Figure 4) deposited at 460 °C on silicon showed that the thicker film had grains with a larger average diameter (2000 Å vs 1100 Å). A cross-sectional view of the 13 000-Å film (Figure 4 inset) showed it had a columnar structure.

UV−vis transmission spectra for ≈3000-Å films grown on quartz are shown in Figure 5. The films prepared at ≥300 °C showed >75% transmittance in the 400−800 nm region. This value is comparable to the ≈80% transmittance (400−800 nm) reported for a 2550-Å film deposited at 450 °C by CVD from tris(acetylacetonato)indium, In[MeC(O)CHC(O)Me]$_3$, and O_2,[8] and the average 83% transmittance found for a 4900-Å film deposited at 500 °C from tris(2,2,6,6-tetramethyl-3,5-heptanedionato)indium, In[*t*-BuC(O)CHC(O)-*t*-Bu]$_3$, and O_2/H_2O.[6] Optical-band gaps were calculated from the absorbance data by plotting α^2 vs E and extrapolating the linear portion of the curve to $\alpha^2 = 0$, where α is the absorption coefficient and E is the photon energy. At $T_{dep} = 300$, 380, and 500 °C, the band gaps were 3.89, 3.86, and 3.77 eV, respectively. These values are close to those reported previously for undoped In_2O_3 films prepared by CVD (3.5−3.8 eV).[7,8,12,15,20]

Resistivities for 3000−3600-Å films deposited on silicon and glass at 300−500 °C ranged from 1.1×10^{-3} to 9×10^{-4} Ω cm (Table 4). The resistivities decreased slightly with increasing deposition temperature up to 460 °C. The lowest resistivity reported previously for an undoped indium oxide film prepared by CVD was 9.3×10^{-4} Ω cm. It was deposited at 508 °C by using trimethylindium diethyl etherate and O_2 as precursors in an atmospheric pressure process.[20]

Conclusion

The amide complex In[N-*t*-Bu(SiMe$_3$)]$_3$ is a convenient starting material for the synthesis of homoleptic indium alkoxide compounds. The complexes of the sterically demanding ligands O-*t*-Bu, OCMe$_2$Et, OCMeEt$_2$, and OCMe$_2$-*i*-Pr are simple edge-shared tetrahedral dimers, but the isopropoxide derivative is an insoluble, presumably polymeric, compound, and the 3-pentoxide derivative is a tetramer. In reactions with certain alcohols, a possible complication with the use of In[N-*t*-Bu(SiMe$_3$)]$_3$ is the generation of *t*-BuNH$_2$, such as in the reaction that forms In(O-2,6-*i*-Pr$_2$C$_6$H$_3$)$_3$(H$_2$N-*t*-Bu)$_2$. The present results and our previous observations suggest that if *t*-BuNH$_2$ is to be avoided in reactions between In[N-*t*-Bu(SiMe$_3$)]$_3$ and ROH or, more generally, X−H reagents, pK_a(X−H) should be >10−11. The homoleptic alkoxide dimers do not form stable pyridine adducts, but the powerful donor *p*-(dimethylamino)pyridine disrupts the dimers [In(μ-OR)(OR)$_2$]$_2$ (R = *t*-Bu and CMeEt$_2$) to form, respectively, four- and five-coordinate complexes. The complex [In(μ-O-*t*-Bu)(O-*t*-Bu)$_2$]$_2$ also reacted with 2,2,6,6-tetramethyl-3,5-heptanedione to yield (*t*-BuO)$_2$In(μ-O-*t*-Bu)$_2$In(*t*-Bu$_2$-β-diketonate)$_2$, which has four- and six-coordinate indium centers and C_2 symmetry. The formation of the 2,2,6,6-tetramethyl-3,5-heptanedionate complex suggests other β-diketonate complexes will also be accessible via the same synthetic route, including perhaps monomeric derivatives akin to Al(OSiPh$_3$)$_2$-(acac).[40]

The primary purpose of this work was to synthesize indium alkoxide complexes for use as chemical vapor deposition precursors to doped and undoped indium oxide films. Of the compounds reported here, [In(μ-OCMe$_2$Et)(OCMe$_2$Et)$_2$]$_2$ was the best precursor candidate because of its favorable physical properties. Low-pressure chemical vapor deposition using [In(μ-OCMe$_2$Et)(OCMe$_2$Et)$_2$]$_2$ and O_2 as precursors yielded conductive (100)-oriented cubic indium oxide films at substrate temperatures of 300−500 °C. Backscattering spectrometry and X-ray photoelectron spectroscopy studies indicated that the films were virtually carbon-free. The lowest resistivity, 9.1×10^{-4} Ω cm, was obtained for the film deposited at 460 °C. This value is among the lowest reported resistivities for undoped indium oxide films. Studies to prepare doped indium oxide films are in progress.

Experimental Section

General. All manipulations were carried out in a glovebox or by using standard Schlenk techniques. Solvents were purified by using standard techniques, after which they were stored in the glovebox over 4-Å molecular sieves. The alcohols were purchased from Aldrich. *i*-PrOH was purified by distillation from Mg and the other alcohols were degassed and dried over 4-Å molecular sieves before use. 4-(Dimethylamino)pyridine was purchased from Acros and used as received. In[N-*t*-Bu(SiMe$_3$)]$_3$ was prepared according to the literature method.[28] NMR spectra were collected on a 300-MHz instrument. Elemental analyses were performed by Oneida Research Services (Whitesboro, NY) and Midwest Microlab (Indianapolis, IN).

[In(μ-O-*t*-Bu)(O-*t*-Bu)$_2$]$_2$ (1). *t*-BuOH (0.21 g, 2.8 mmol) was added dropwise via a pipet to a solution of In[N-*t*-Bu(SiMe$_3$)]$_3$ (0.50 g, 0.91 mmol) in hexanes (20 mL) at room temperature. After 15 h of stirring, the volatile components were distilled in vacuo. The resulting white solid was extracted with hexanes (15 mL), and the extract was filtered over Celite. The colorless filtrate was concentrated to 1 mL, and then cooled in the freezer (−35 °C) overnight. Colorless crystalline blocks formed, which were isolated by decanting the mother liquor (yield 0.25 g, 82%). Anal. Calcd for $C_{24}H_{54}O_6In_2$: C, 37.69; H, 7.12. Found: C, 37.51; H, 7.14. ^{1}H NMR ($CDCl_3$): δ 1.50 (s, 18, μ-OC*Me*$_3$), 1.32 (s, 36, OC*Me*$_3$.). ^{13}C{^{1}H} NMR (C_6D_6): 76.2 (2, μ-O*C*Me$_3$), 71.9 (4, O*C*Me$_3$), 35.4 (12, OC*Me*$_3$), 33.7 (6, μ-OC*Me*$_3$.). IR (Nujol, KBr, cm^{-1}):

1395 (m), 1370 (s), 1360 (s), 1236 (s), 1223 (s), 1186 (s), 1032 (w), 1022 (w), 957 (s), 905 (s), 760 (s).

[In(OCMe$_2$Et)$_2$(μ-OCMe$_2$Et)]$_2$ (2). EtMe$_2$COH (0.15 g, 1.70 mmol) was added dropwise via a pipet to a solution of In[N-*t*-Bu(SiMe$_3$)]$_3$ (0.30 g, 0.55 mmol) in ether (15 mL) at room temperature. After 15 h of stirring, the volatile components were distilled in vacuo. Sublimation from the resulting white solid (95−110 °C, 10^{-2} mmHg) yielded the product as a colorless solid (mp 40−42 °C) on the coldfinger (yield 0.19 g, 91%). Anal. Calcd for $C_{30}H_{66}O_6In_2$: C, 47.88; H, 8.84. Found: C, 47.91; H, 9.05. ^{1}H NMR (C_6D_6): δ 1.82 (q, 4, ^3J = 7 Hz, μ-OC(CH$_3$)$_2$C*H*$_2$CH$_3$), 1.69 (q, 8, ^3J = 7 Hz, OC(CH$_3$)$_2$C*H*$_2$CH$_3$), 1.49 (s, 12, μ-OC(C*H*$_3$)$_2$CH$_2$CH$_3$), 1.43 (s, 24, OC(C*H*$_3$)$_2$CH$_2$CH$_3$), 1.08 (t, 12, ^3J = 7 Hz, OC(CH$_3$)$_2$CH$_2$C*H*$_3$), 0.88 (t, 6, ^3J = 7 Hz, μ-OC(CH$_3$)$_2$CH$_2$C*H*$_3$). ^{13}C{^{1}H} NMR (C_6D_6): 78.7 (2, μ-O*C*(CH$_3$)$_2$CH$_2$CH$_3$), 73.8 (4, O*C*(CH$_3$)$_2$CH$_2$CH$_3$), 40.0 (4, OC(CH$_3$)$_2$*C*H$_2$CH$_3$), 39.9 (2, μ-OC(CH$_3$)$_2$*C*H$_2$CH$_3$), 33.1 (8, OC(*C*H$_3$)$_2$CH$_2$CH$_3$), 30.6 (4, μ-OC(*C*H$_3$)$_2$CH$_2$CH$_3$), 10.3 (2, μ-OC(CH$_3$)$_2$CH$_2$*C*H$_3$), 10.0 (4, OC(CH$_3$)$_2$CH$_2$*C*H$_3$). IR (Nujol, KBr, cm^{-1}): 1360 (s), 1289 (m), 1225 (m), 1170 (s), 1154 (s), 1059 (s), 1018 (w), 964 (s), 934 (s), 878 (s), 735 (s).

[In(μ-OCMeEt$_2$)(OCMeEt$_2$)$_2$]$_2$ (3). Et$_2$MeCOH (0.65 g, 6.4 mmol) was added dropwise via a pipet to a solution of In[N-*t*-Bu(SiMe$_3$)]$_3$ (0.50 g, 0.91 mmol) in ether (15 mL) at room temperature. After 2 d of stirring, the volatile components were distilled in vacuo. The resulting sticky white solid was extracted with hexanes (15 mL). The extract was filtered over Celite, and then the hexanes were removed in vacuo from the filtrate. Sublimation from the sticky white solid residue (135−150 °C, 10^{-2} mmHg) yielded the product as a sticky white solid on the coldfinger (yield 0.35 g, 92%). The compound was very difficult to handle. A satisfactory analysis was not obtained. Anal. Calcd for $C_{36}H_{78}O_6In_2$: C, 51.68; H, 9.40. Found: C, 49.75; H, 8.90. ^{1}H NMR (C_6D_6): δ 1.58−1.90 (m, 24, μ-OCMe(C*H*$_2$CH$_3$)$_2$, OCMe(C*H*$_2$CH$_3$)$_2$), 1.50 (s, 6, μ-OC*Me*Et$_2$), 1.41 (s, 12, OC*Me*Et$_2$), 1.04 (t, 24, ^3J = 7 Hz, OCMe(CH$_2$C*H*$_3$)$_2$), 0.96 (t, 12, ^3J = 7 Hz, μ-OCMe(CH$_2$C*H*$_3$)$_2$). ^{13}C{^{1}H} NMR (C_6D_6): 80.6 (2, μ-O*C*MeEt$_2$), 75.7 (4, O*C*MeEt$_2$), 37.1 (8, OCMe(*C*H$_2$CH$_3$)$_2$), 36.2 (4, μ-OCMe(*C*H$_2$CH$_3$)$_2$), 31.0 (4, OC*Me*Et$_2$), 28.3 (2, μ-OC*Me*Et$_2$), 9.7 (8, OCMe(CH$_2$*C*H$_3$)$_2$), 9.6 (4, μ-OCMe(CH$_2$*C*H$_3$)$_2$). IR (Nujol, KBr, cm^{-1}): 1337 (w), 1323 (w), 1292 (w), 1273 (w), 1217 (w), 1150 (s), 1063 (m), 1036 (m), 984 (s), 924 (s), 889 (s), 775 (w), 718 (m).

[In(μ-OCMe$_2$-*i*-Pr)(OCMe$_2$-*i*-Pr)$_2$]$_2$ (4). *i*-PrMe$_2$COH (0.65 g, 6.4 mmol) was added dropwise via a pipet to a solution of In[N-*t*-Bu(SiMe$_3$)]$_3$ (0.50 g, 0.91 mmol) in ether (15 mL) at room temperature. After 2 d of stirring, the volatile components were distilled in vacuo. The resulting white solid was extracted with hexanes (15 mL). The extract was filtered over Celite, and the hexanes were distilled from the filtrate in vacuo. Sublimation from the white solid residue (135−150 °C, 10^{-2} mmHg) yielded the product as a white solid on the coldfinger (yield 0.34 g, 89%). Anal. Calcd for $C_{36}H_{78}O_6In_2$: C, 51.68; H, 9.40. Found: C, 51.31; H, 9.19. ^{1}H NMR (C_6D_6): δ 1.96 (septet, 2, ^3J = 7 Hz, μ-OC(CH$_3$)$_2$C*H*(CH$_3$)$_2$), 1.81 (septet, 4, ^3J = 7 Hz, OC(CH$_3$)$_2$C*H*(CH$_3$)$_2$), 1.49 (s, 12, μ-OC(C*H*$_3$)$_2$CH(CH$_3$)$_2$), 1.42 (s, 24, OC(C*H*$_3$)$_2$CH(CH$_3$)$_2$), 1.11 (d, 24, ^3J = 7 Hz, OC(CH$_3$)$_2$CH(C*H*$_3$)$_2$), 0.99 (d, 12, ^3J = 7 Hz, μ-OC(CH$_3$)$_2$CH(C*H*$_3$)$_2$). ^{13}C{^{1}H} NMR (C_6D_6): 80.8 (2, μ-O*C*(CH$_3$)$_2$CH(CH$_3$)$_2$), 75.6 (4, O*C*(CH$_3$)$_2$CH(CH$_3$)$_2$), 42.3 (2, μ-OC(CH$_3$)$_2$*C*H(CH$_3$)$_2$), 41.3 (4, OC(CH$_3$)$_2$*C*H(CH$_3$)$_2$), 31.4 (8, OC(*C*H$_3$)$_2$CH(CH$_3$)$_2$), 28.2 (4, μ-OC(*C*H$_3$)$_2$CH(CH$_3$)$_2$), 19.1 (4, μ-OC(CH$_3$)$_2$CH(*C*H$_3$)$_2$), 18.7 (8, OC(CH$_3$)$_2$CH(*C*H$_3$)$_2$). IR (Nujol, KBr, cm^{-1}): 1370 (s), 1321 (w), 1238 (w), 1217 (w), 1196 (m), 1165 (s), 1146 (s), 1099 (s), 1063 (w), 1053 (m), 968 (s), 951 (s), 905 (s), 853 (s), 710 (s).

In[(μ-OCHEt$_2$)$_2$In(OCHEt$_2$)$_2$]$_3$ (5). Et$_2$CHOH (0.53 g, 6.0 mmol) was added dropwise via a pipet to a solution of In[N-*t*-Bu(SiMe$_3$)]$_3$ (1.0 g, 1.8 mmol) in hexanes (20 mL). After18 h of stirring, the volatile components were removed in vacuo. During the distillation, the compound crystallized as colorless thick plates (yield 0.62 g, 90%). The compound can be recrystallized from a hexanes solution at low temperature if desired. Anal. Calcd for $C_{60}H_{132}O_{12}In_4$: C, 47.89; H, 8.84. Found: C, 47.75; H, 8.82. ^{1}H NMR (C_6D_6): δ 4.33 (m, 6, OC*H*Et$_2$), 4.00 (m, 6, OC*H*Et$_2$), 1.6−2.4 (m, 48, OCH(C*H*$_2$CH$_3$)$_2$), 1.15 (t, 18, ^3J = 7 Hz, OCH(CH$_2$C*H*$_3$)$_2$), 1.06 (overlapping t, 54, OCH(CH$_2$C*H*$_3$)$_2$). ^{13}C{^{1}H} NMR (C_6D_6): 78.6 (6, O*C*HEt$_2$), 77.0 (6, O*C*HEt$_2$), 32.6 (6, OCH(*C*H$_2$CH$_3$)$_2$), 32.4 (6, OCH(*C*H$_2$CH$_3$)$_2$), 31.8 (6, OCH(*C*H$_2$CH$_3$)$_2$), 30.3 (6, OCH(*C*H$_2$CH$_3$)$_2$), 10.4 (6, OCH(CH$_2$*C*H$_3$)$_2$), 10.3 (6, OCH(CH$_2$*C*H$_3$)$_2$), 9.7 (6, OCH(CH$_2$*C*H$_3$)$_2$), 9.3 (6, OCH(CH$_2$*C*H$_3$)$_2$). IR (Nujol, KBr, cm^{-1}): 1350 (m), 1307 (w), 1155 (w), 1125 (s), 1111 (s), 1044 (s), 1015 (w), 988 (s), 953 (s), 918 (m), 856 (w).

[In(O-*i*-Pr)$_3$]$_n$ (6). *i*-PrOH (0.34 g, 5.6 mmol) was added dropwise via pipet to a solution of In[N-*t*-Bu(SiMe$_3$)]$_3$ (1.0 g, 1.8 mmol) in hexanes (15 mL). The solution became cloudy during the addition. After 1.5 h of stirring, the mixture was filtered. The solid collected on the frit was washed with hexanes (15 mL) and ether (15 mL) and then dried in vacuo (yield 0.48 g, 90%). Anal. Calcd for $C_9H_{21}O_3In$: C, 37.01; H, 7.25. Found: C, 36.77; H, 7.18. IR (Nujol, KBr, cm^{-1}): 1383 (m), 1341 (m), 1171 (m), 1123 (s), 961 (s), 837 (s).

In(O-2,6-*i*-Pr$_2$C$_6$H$_3$)$_3$(H$_2$N-*t*-Bu)$_2$ (7). 2,6-*i*-Pr$_2$C$_5$H$_3$OH (0.49 g, 2.8 mmol) in ether (5 mL) was added dropwise to a solution of In[N-*t*-Bu(SiMe$_3$)]$_3$ (0.30 g, 0.55 mmol) in ether (30 mL) at room temperature. After 15 h of stirring, the volatile components were distilled in vacuo. The resulting viscous yellow oil was extracted with hexanes (20 mL), and the extract was filtered. The yellow filtrate was concentrated to 3 mL, and toluene (1 mL) was added. When the solution was cooled to −35 °C, the product formed as colorless crystals (yield 0.23 g, 53%). Anal. Calcd for $C_{44}H_{73}N_2O_3In$: C, 66.65; H, 9.28; N, 3.53. Found: C, 66.41; H, 9.27; N, 3.49. ^{1}H NMR (C_6D_6): δ 7.15 (d, 6, ^3J = 7.6 Hz, *m*-Ph), 6.94 (t, 3, *p*-Ph), 3.58 (septet, 6, ^3J = 7.6 Hz, C*H*Me$_2$), 2.83 (br s, 4, *H*$_2$N-*t*-Bu), 1.24 (d, 36, ^3J = 7.6 Hz, CH*Me*$_2$), 0.99 (s, 18, H$_2$NC*Me*$_3$). ^{13}C{^{1}H} NMR (C_6D_6): 157.7 (3, *ipso*-Ph), 138.6 (6, *o*-Ph), 123.6 (6, *m*-Ph), 119.0 (3, *p*-Ph), 51.3 (2, H$_2$N*C*Me$_3$), 29.8, 27.7 (6 each, *C*HMe$_2$ and H$_2$NC*Me*$_3$), 23.9 (12, CH*Me*$_2$). IR (Nujol, KBr, cm^{-1}): 3312 (s), 3231 (s), 1588 (m), 1568 (m), 1427 (s), 1398 (w), 1360 (m), 1325 (s), 1254 (s), 1204 (s), 1142 (m), 1111 (s), 1043 (m), 1018 (m), 932 (m), 897 (m), 883 (m), 847 (s), 797 (w), 756 (s), 683 (m), 627 (m), 611 (w).

In(O-*t*-Bu)$_3$(*p*-Me$_2$Npy)$_2$ (8). 4-(Dimethylamino)pyridine (0.073 g, 0.60 mmol) was added at room temperature to an ether (10 mL) solution of [In(O-*t*-Bu)$_3$]$_2$ (0.10 g, 0.15 mmol). After 30 min of stirring, the ether was concentrated in vacuo to 2 mL. The flask was then placed in the freezer (−35 °C). Fragile colorless needles formed overnight, which were isolated by decanting the mother liquor (yield 0.14 g, 81%). Anal. Calcd for $C_{26}H_{47}N_4O_3In$: C, 53.98; H, 8.19; N 9.69. Found: C, 53.68; H, 7.58; N, 9.78. ^{1}H NMR (C_6D_6): δ 8.43 (d, 4, *o*-Ph), 5.92 (d, 4, *m*-Ph), 2.12 (s, 12, N*Me*$_2$), 1.71 (s, 27, OC*Me*$_3$). ^{13}C{^{1}H} NMR (C_6D_6): 154.4 (4, 4-py), 149.6 (4, 2-py), 106.8 (4, 3-py), 70.4 (3, O*C*Me$_3$), 38.2 (4, N*Me*$_2$), 35.4 (9, OC*Me*$_3$). IR (Nujol, KBr, cm^{-1}): 1611 (s), 1537 (s), 1352 (m), 1225 (s), 1194 (s), 1117 (w), 1071 (w), 1007 (s), 988 (m), 974 (s), 947 (s), 810 (s), 721 (w).

In(OCMeEt$_2$)$_3$(*p*-Me$_2$Npy) (9). 4-(Dimethylamino)pyridine (0.03 g, 0.24 mmol) was added at room temperature to an ether (10 mL) solution of [In(OCMeEt$_2$)$_2$(μ-OCMeEt$_2$)]$_2$ (0.10 g, 0.12 mmol). After 1 h of stirring, the solvent was distilled from the reaction mixture in vacuo. The resulting white solid residue was dissolved in ether/hexanes (v/v = 1 mL/1 mL), and the flask was then placed in the freezer (−35 °C). Fragile colorless thin plates formed overnight, which were isolated by decanting the mother liquor (yield 0.094 g, 73%). Anal. Calcd for $C_{25}H_{49}N_2O_3In$: C, 55.55; H, 9.14; N 5.18. Found: C, 55.88; H, 9.06; N, 5.19. ^{1}H NMR (C_6D_6): δ 8.42 (d, 2, *o*-Ph), 5.68 (d, 2, *m*-Ph), 1.92 (s, 6, N*Me*$_2$), 1.88 (q, 12, ^3J = 7 Hz, OCMe(C*H*$_2$CH$_3$)$_2$), 1.58 (s, 9, OC*Me*Et$_2$), 1.19 (t, 18, ^3J = 7 Hz, OCMe(CH$_2$C*H*$_3$)$_2$). ^{13}C{^{1}H} NMR (C_6D_6): 155.0 (1, 4-py), 148.4 (2, 2-py), 106.7 (2, 3-py), 73.9 (3, O*C*MeEt$_2$), 38.1 (2, N*Me*$_2$), 37.1 (6, OCMe(*C*H$_2$CH$_3$)$_2$), 30.6 (3, OC*Me*Et$_2$), 9.7 (6, OCMe(CH$_2$*C*H$_3$)$_2$). IR (Nujol, KBr, cm^{-1}): 1626 (s), 1547 (s), 1395 (m), 1366 (m), 1296 (w), 1271 (w), 1231 (s), 1175 (m), 1152 (s), 1117 (w), 1071 (s), 1017 (s), 1001 (s), 980 (s), 949 (w), 922 (s), 883 (w), 814 (s), 760 (w).

(*t*-BuO)$_2$In(μ-O-*t*-Bu)$_2$In(*t*-Bu$_2$-β-diketonate)$_2$ (10). *t*-Bu$_2$-β-diketone (0.17 g, 0.90 mmol) was added dropwise to a solution of [In(O-*t*-Bu)$_3$]$_2$ (0.30 g, 0.45 mmol) in benzene (10 mL) at room temperature. The flask was closed off and placed in an oil bath at 80 °C for 15 h (CAUTION: CLOSED FLASK HEATING). The volatile components were then removed in vacuo. The resulting white solid was extracted with hexanes (15 mL), and the extract was filtered. The colorless filtrate

was taken to dryness under vacuum, and toluene (2 mL) was added to the residue. The flask was placed in the freezer (−35 °C). The product crystallized under these conditions as fragile colorless needles, which were isolated by decanting the mother liquor (yield 0.32 g, 80%). Anal. Calcd for $C_{38}H_{74}O_8In_2$: C, 51.36; H, 8.39. Found: C, 51.29; H, 8.38. ^{1}H NMR (C_6D_6): δ 5.76 (s, 2, $Me_3CC(O)CHC(O)CMe_3$), 1.64 (s, 18, μ-OCMe_3), 1.56 (s, 18, OCMe_3), 1.17 (s, 36, $Me_3CC(O)CHC(O)CMe_3$). ^{13}C{^{1}H} NMR (C_6D_6): 204 (4, $Me_3CC(O)CH_2C(O)CMe_3$), 90.5 (2, $Me_3CC(O)CHC(O)CMe_3$), 74.2 (2, OCMe_3), 71.5 (2, μ-OCMe_3), 41.9 (4, $Me_3CC(O)CHC(O)CMe_3$), 35.5 (6, μ-OCMe_3), 33.1 (6, OCMe_3), 28.4 (12, $Me_3CC(O)CHC(O)CMe_3$). IR (Nujol, KBr, cm^{-1}): 1595 (m), 1572 (s), 1551 (s), 1507 (s), 1398 (s), 1381 (s), 1358 (s), 1246 (w), 1227 (m), 1186 (m), 1138 (m), 1026 (w), 961 (w), 941 (w), 907 (m), 872 (m), 795 (m), 758 (w), 741 (w).

X-ray Crystallography. Crystals of [In(μ-O-*t*-Bu)(O-*t*-Bu)$_2$]$_2$ (**1**), In[(μ-OCHEt$_2$)$_2$In(OCHEt$_2$)$_2$]$_3$ (**5**), [In(O-*i*-Pr$_2$C$_6$H$_3$)$_3$(H$_2$N-*t*-Bu)$_2$]$_2$·1/2C$_7$H$_9$ (**7**·1/2C$_7$H$_9$), [In(O-*t*-Bu)$_3$(*p*-Me$_2$Npy)$_2$]$_2$·1/2Et$_2$O (**8**·1/2Et$_2$O), In(OCMeEt$_2$)$_3$(*p*-Me$_2$Npy) (**9**), and (*t*-BuO)$_2$In(μ-O-*t*-Bu)$_2$In(*t*-Bu$_2$-β-diketonate)$_2$ (**10**) are colorless triangular plates (**1**), thick plates (**5**, **9**, and **8**·1/2Et$_2$O), parallelepipeds (**7**·1/2C$_7$H$_9$), and prismatic columns (**10**). Crystals of **1** were prepared by heating a saturated hexanes solution of the compound in an oil bath (bath temp. ≈60 °C) and then slowly cooling the solution to room temperature. Compound **5** crystallized from hexanes as the volume of a hexanes solution was being reduced in vacuo. Crystals of **7**·1/2C$_7$H$_9$, **8**·Et$_2$O, **9**, and **10** were obtained from cold (−35 °C) solutions of toluene/hexanes, ether, ether/hexanes and toluene, respectively. Data were collected on a Siemens SMART CCD instrument. Some relevant details concerning the crystallographic studies follow:

1: The Laue symmetry was determined to be −1, and the space group was shown to be *P*1 or *P*-1. One of the *tert*-butyl groups was found to be disordered over two different orientations, with 50:50 occupancy.

5: The Laue symmetry was determined to be 2/*m*, and from the systematic absences noted, the space group was shown unambiguously to be $P2_1/c$. The majority of the alkoxide ligands were found to be disordered, and this was treated by employing distance constraints.

7·1/2C$_7$H$_9$: The Laue symmetry was determined to be 2/*m*, and from the systematic absences noted, the space group was shown to be *Cc* or *C*2/*c*. The disordered toluene methyl hydrogens were located in a difference map and held fixed, but the amine hydrogens were allowed to refine independently.

8·1/2Et$_2$O: The Laue symmetry was determined to be −1, and the space group was shown to be *P*1 or *P*-1. All three of the equatorial alkoxide ligands were disordered over two slightly different orientations, and the ether solvent was disordered about an inversion center.

9: The Laue symmetry was determined to be 2/*m*, and from the systematic absences noted, the space group was shown unambiguously to be $P2_1/c$.

10: The Laue symmetry was determined to be 2/*m*, and from the systematic absences noted, the space group was shown to be *Cc* or *C*2/*c*. The structure was massively disordered. The disorder was not removed by refinement in the lower symmetry space group *Cc*. The primary disorder involves the two β-diketonate ligands on In2. At each site, there is a 50:50 mix of the molecule shown in Scheme 2 and its enantiomer. Within each molecule, there are also two disordered tert-butyl groups, both of which were treated using ideal rigid bodies. The C5:C5′:C5″ orientations were found to have occupancies of 40%:33%:27%, and the C16′:C16″ orientations were found to have occupancies of 37%:13%. Two large peaks appeared in the difference density map separated by a distance equal to the In1−In2 distance. This is presumed to be a minor directional disorder of the molecules along the 2-fold axis. Reasonable thermal parameters were obtained when the populations of In1′ and In2′ were fixed at 2%.

Film Depositions and Characterization. Depositions were performed using a simple home-built horizontal hot-wall low-pressure CVD system equipped with mass-flow controllers. The precursor container was maintained at 53−55 °C. During depositions, five different sections of the precursor feed lines were maintained at temperatures ranging from 74 to 160 °C. The argon (UHP grade) carrier gas flow rate through the precursor container was 500 sccm. The oxygen (extra dry grade;150 sccm) was diluted in argon (600 sccm) before entering the reactor.

Ion beam data were collected by Dr. Yongqiang Wang at the Ion Beam Analysis Facility, University of Minnesota. The beam was 2-MeV $^4He^+$ ions, and the total charge collected for the spectrum was 10 μC at 10 nA. The RBS detector (fwhm = 18 keV, Ω = 4.16 msr) was located at 165°. X-ray diffraction studies were performed using Siemens diffractometers (Cu Kα radiation; 0.01° step size), and X-ray photoelectron spectroscopy studies were carried out using a system (Physical Electronics, PHI 5700 ESCA) equipped with a 5-keV Ar^+ sputter gun. The electron-energy analyzer was referenced to the Au $4f_{7/2}$ line at 84 eV. XP spectra during depth-profile analyses were collected using a standard Al Kα source. The width was set at 11.75 eV throughout. The base pressure was 2×10^{-8} Torr during sputtering. After sputtering into the bulk, spectra were collected using a monochromated Al source at a pass energy of 11.75 eV. The base pressure was below 10^{-9} Torr.

Sheet resistances were measured for films deposited on silicon (the substrate resistivity was 30 Ω cm) and glass by using a four-point probe configuration (Signatone model S-301). A series of 3−4 measurements were taken on each film, and the measurements then were averaged to give the final reported value. Variations of ±2% in the individual measurements were typically observed. Film thicknesses were obtained from SEM (JEOL JSM-6330F) cross-sectional views.

Acknowledgment. Acknowledgment for technical assistance with the crystal structure determinations is made to Dr. James Korp. This work was supported in part by the Robert A. Welch Foundation, by the MRSEC Program of the National Science Foundation under Award Number DMR-9632667, and by the State of Texas through the Texas Center for Superconductivity at the University of Houston and the Advanced Research Program.

Supporting Information Available: Six X-ray crystallographic files, in CIF format. This material is available free of charge via the Internet at http://pubs.acs.org.

JA000845A